

Supplementary Tables and Figures for the manuscript:

A dimerization-based fluorogenic dye-aptamer module for RNA imaging in live cells

Farah Bouhedda^{1,3}, Kyong Tkhe Fam^{2,3}, Mayeul Collot^{2*}, Alexis Autour¹, Stefano Marzi¹, Andrey Klymchenko^{2,4*} & Michael Ryckelynck^{1,4*}

1. Université de Strasbourg, CNRS, Architecture et Réactivité de l'ARN, UPR 9002, F-67000 Strasbourg, France

2. Nanochemistry and Bioimaging group, Laboratoire de Bioimagerie et Pathologies, CNRS UMR 7021, Université de Strasbourg, 67401 Illkirch, France

3. These authors equally contributed to this work

4. Co-last authors

* mayeul.collot@unistra.fr; andrey.klymchenko@unistra.fr; m.ryckelynck@unistra.fr

Supplementary Table 1 | Affinity between RNA aptamers and Sulforhodamine B, Gemini-561 or its alkyne derivative.

Dye/RNA couple	K_D affinity constant
Sulforhodamine B/SRB2 ^a	310 ± 60.0 nM
Sulforhodamine B/o-Coral	> 400 nM
Gemini-561/SRB2	441 ± 167.5 nM
Gemini-561/o-Coral	73 ± 1.5 nM
Gemini-561-alkyne/o-Coral	188 ± 2.5 nM

^a As reported in Holeman, L.A., Robinson, S.L., Szostak, J.W. & Wilson, C. Isolation and characterization of fluorophore-binding RNA aptamers. *Fold Des* **3**, 423-31 (1998). K_D values are the mean of n = 3 independent experiments ± 1 SD.

Supplementary Table 2 | Sequence of o-Coral constructs.

Name	Sequence
o-Coral ^a	5' GGGAGACAGCTAGAGTAC CAGAACCCCGCTTCGGCGGTGATGGAGAGGGCGCAAGGTTAACCGCC TCAGGTTCCGGTGACGGGGCCTCGCTTCGGCGATGATGGAGAGGGCGCAAGGTTAACCGCCTCAGG TTCT GACACGAGCACAGTGTAC 3'
o-Coral in F30 scaffold ^{a, b}	5' <i>GTGCTCGCTTCGGCAGCACATATACTAGTCGACT</i> <u>TGCCATGTGTATGTGGGCCTGCAGGGGGA</u> GACAGCTAGAGTAC CAGAACCCCGCTTCGGCGGTGATGGAGAGGGCGCAAGGTTAACCGCCTCAGGT TCCGGTGACGGGGCCTCGCTTCGGCGATGATGGAGAGGGCGCAAGGTTAACCGCCTCAGGTTCT GA CACGAGCACAGTGTAC CCTGCAGGCCACATACTCTGATGATCCTTCGGGATCATTCATGGCAAT <i>CTAGAGCGGACTTCGGTCCGCTTTT</i> 3'

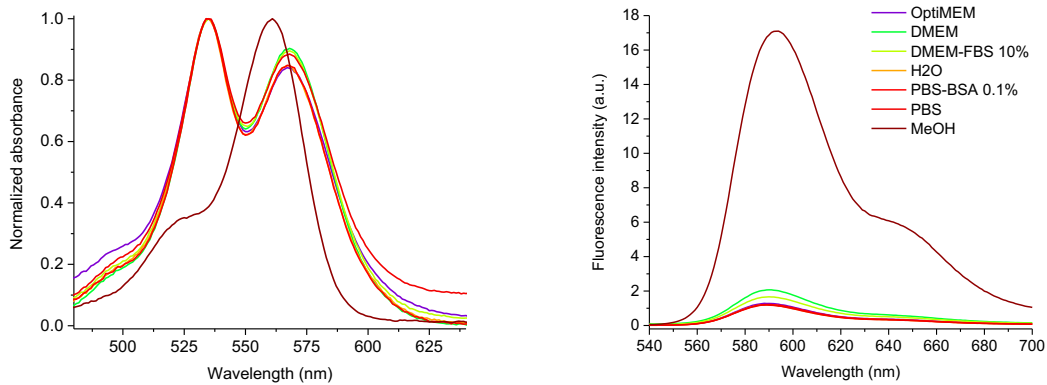
^a The sequence of 5' and 3' extensions are shown in bold. ^b The sequence of the F30 scaffold is underlined. The sequence of 27 first nucleotides of U6 promoter (5' end) and of the U6 terminator (3' end) are italicized.

Supplementary Table 3 | Fluorescence Correlation Spectroscopy (FCS) analysis of the fluoromolecules.^a

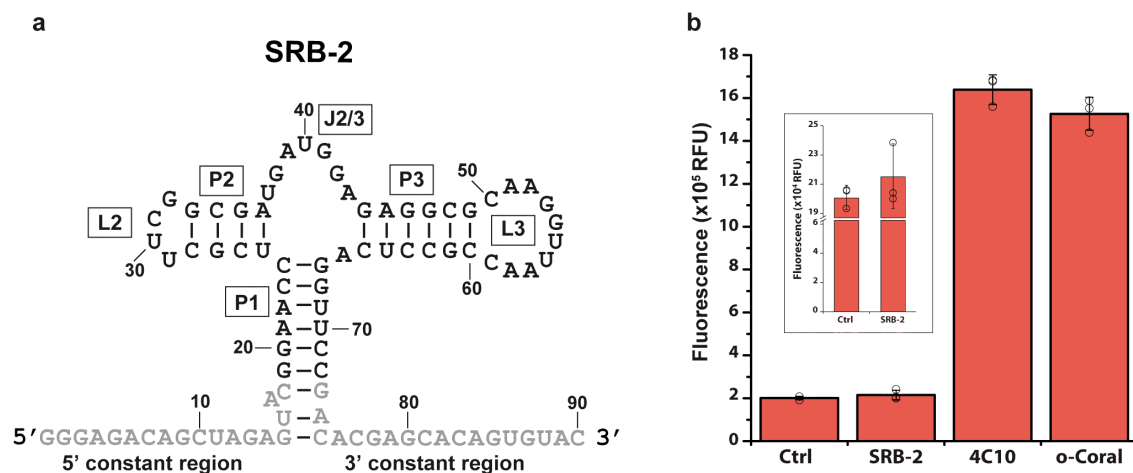
Fluoromolecule/ reference dye	n	τ_{corr} , ms	c, nM	Size, nm	Brightness
Tetramethylrhodamine	11.64	0.032	50	1	1
o-Coral/Gemini-651	43.22	0.22	185.71	6.86	1.14*
RFP	18.2	0.077	84.42	1.53	0.06
mCherry	4.09	0.102	17.54	3.45	0.16
Fluorescein	13.03	0.026	50	1	1
Broccoli/ DFHBI-1T	14.16	0.16	54.35	6.27	0.18
Corn/ DFHO	54.7	0.063	209.94	2.56	0.62
eGFP	20.2	0.075	75.47	2.59	0.16

^an-number of emissive species per excitation volume; τ_{corr} - correlation time; size - hydrodynamic diameter of fluorescent specie; brightness with respect to one molecule of the standard (rhodamine B for o-Coral, fluorescein for Broccoli and Corn). Mango was excluded from this study since its photophysical properties did not fit the analysis settings. Concentrations of fluorogen and corresponding aptamer were systematically 200 nM and 1 μM , respectively.

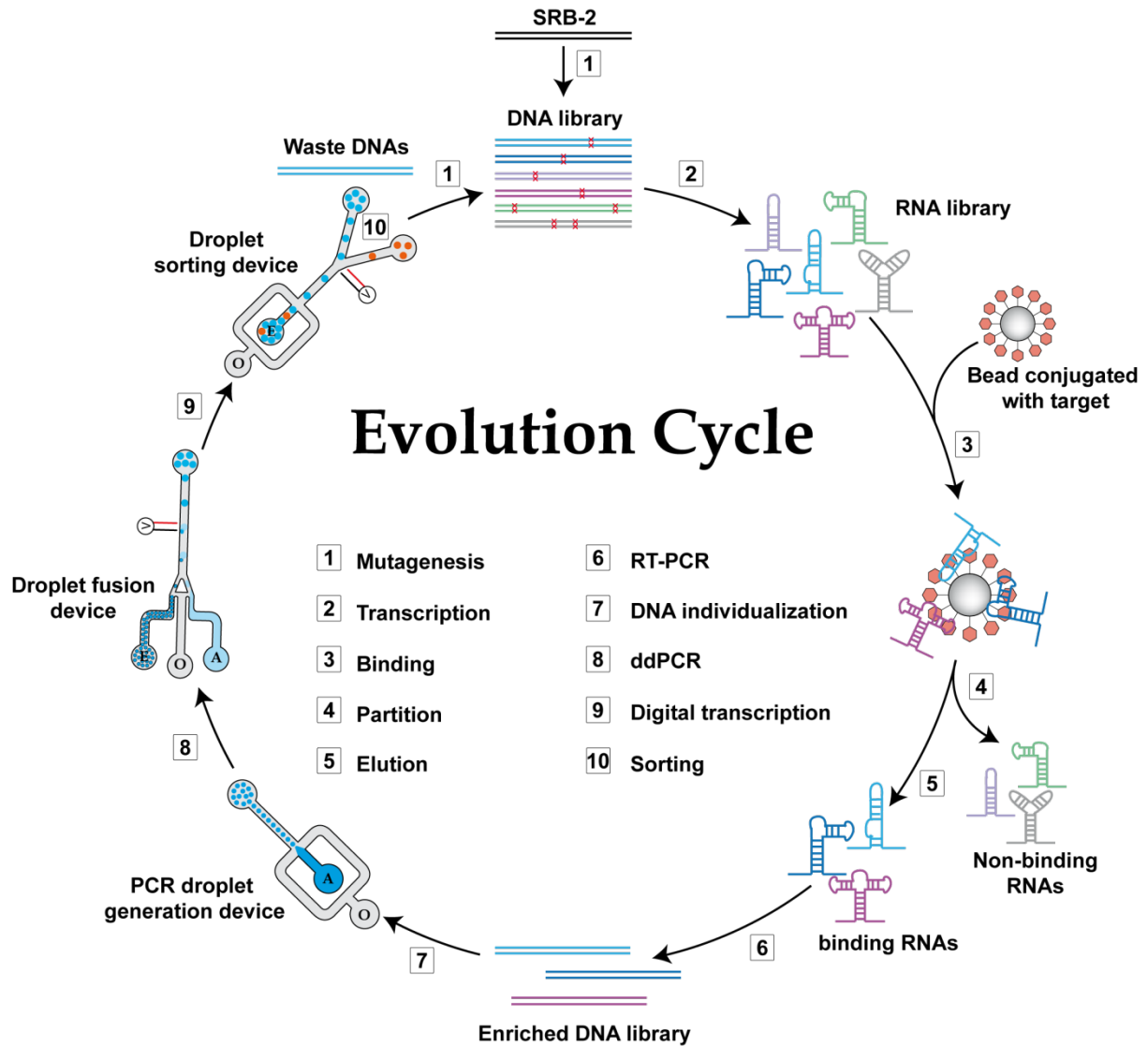
*This value corresponds to 532 nm excitation, which is less efficient for excitation than that for the TMR standard, because of the red shifted absorption of the former.



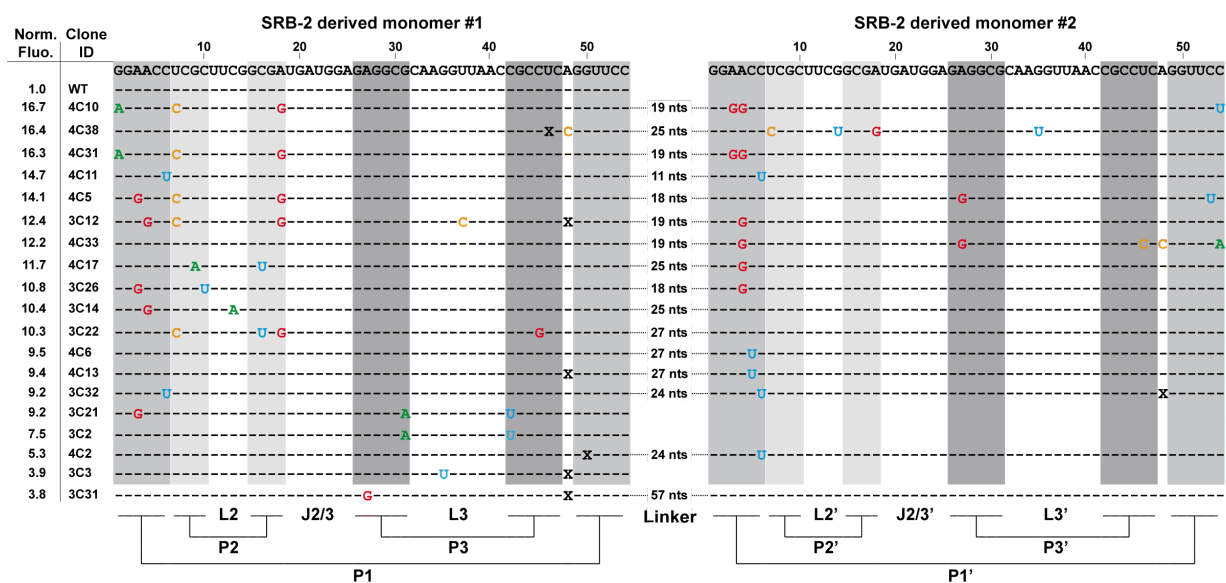
Supplementary Figure 1 | Normalized absorption and emission spectra of Gemini-561 in different aqueous media mimicking cellular environments. Results were found similar in $n = 3$ independent experiments.



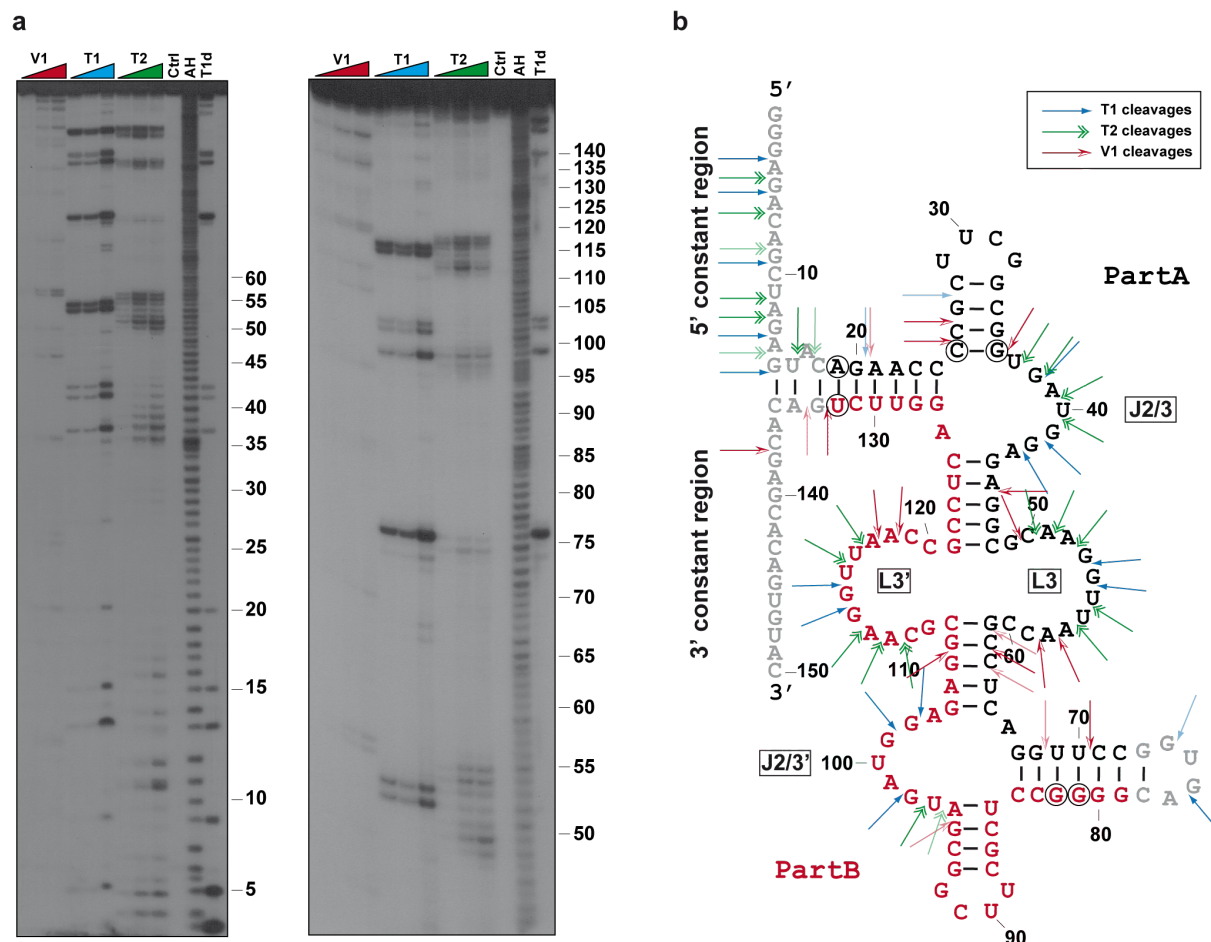
Supplementary Figure 2 | Gemini-561 activation by SRB-2 aptamer and its derivatives. (a) Secondary structure model of SRB-2 aptamer as originally proposed in Holeman, L.A., Robinson, S.L., Szostak, J.W. & Wilson, C. Isolation and characterization of fluorophore-binding RNA aptamers. *Fold Des* **3**, 423-31 (1998). Paired regions (P1, P2 and P3) are distinguished from Loop (L2 and L3) and Junction (J2/3) regions. Constant sequence regions appended for RT-PCR amplification purposes are shown in gray. (b) Fluorogenic capacity of SRB-2 and its evolved forms 4C10 and o-Coral. 500 nM of RNAs were incubated with 50 nM of Gemini-561 and the fluorescence was measured at $\lambda_{ex/em} = 560/600$ nm. The values are the mean of $n = 3$ independent experiments, each measurement being shown as an open circle. The error bars correspond to ± 1 standard deviation.



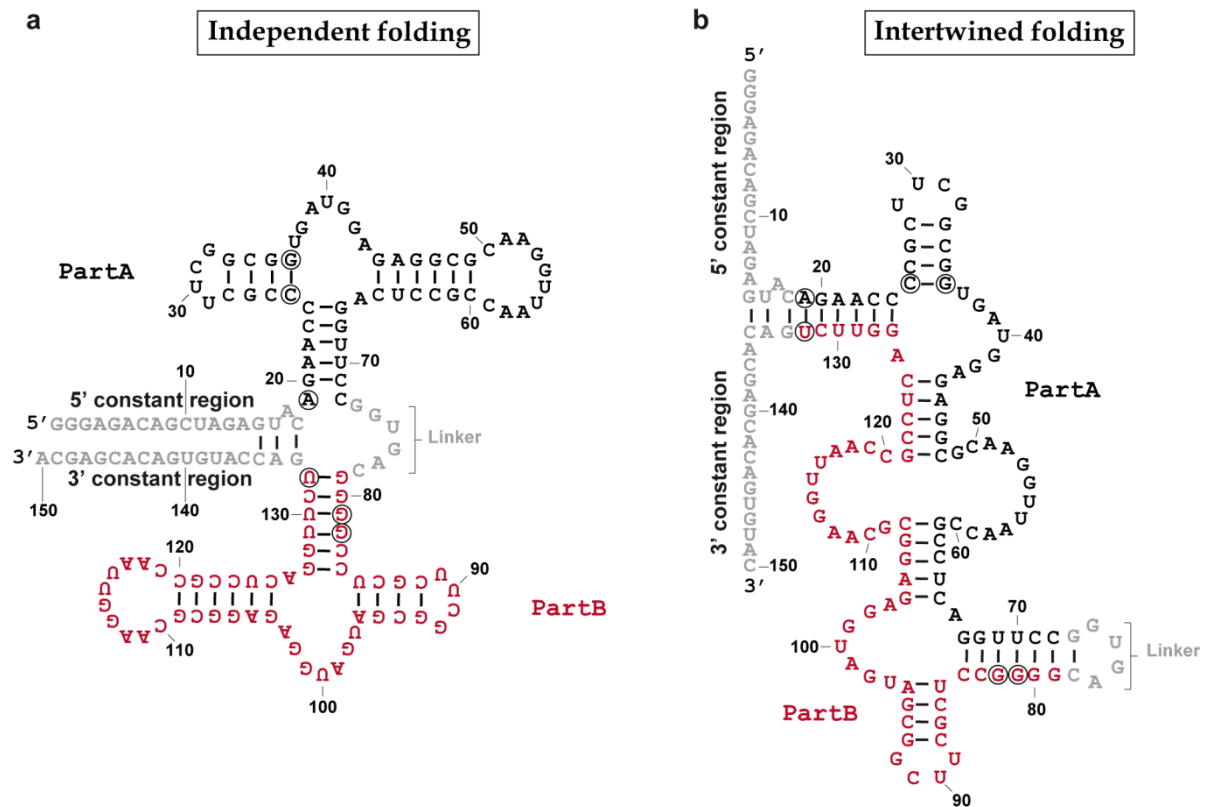
Supplementary Figure 3 | Overall *in vitro* evolution strategy. Each round of evolution cycle consisted of 10 main steps. SRB-2 was used as a template for error-prone PCR (step 1) to create a DNA mutant library that was *in vitro* transcribed (step 2). Resulting RNAs were then selected for their binding capacity *via* a SELEX (Systematic Evolution of Ligands by Exponential enrichment) approach (steps 3, 4 and 5) prior to being screened for their light-up capacity using μ IVC (steps 7, 8, 9 and 10). For steps performed in microfluidic chips, Oil (O) and Aqueous phase (A) inlets are labeled together with inlets and outlets where Emulsion (E) were respectively reinjected and collected. Finally, the enriched pool was reamplified by an error-prone PCR (Step 1) before re-entering the whole process again. 4C10 was obtained after 4 rounds of this evolution cycle.



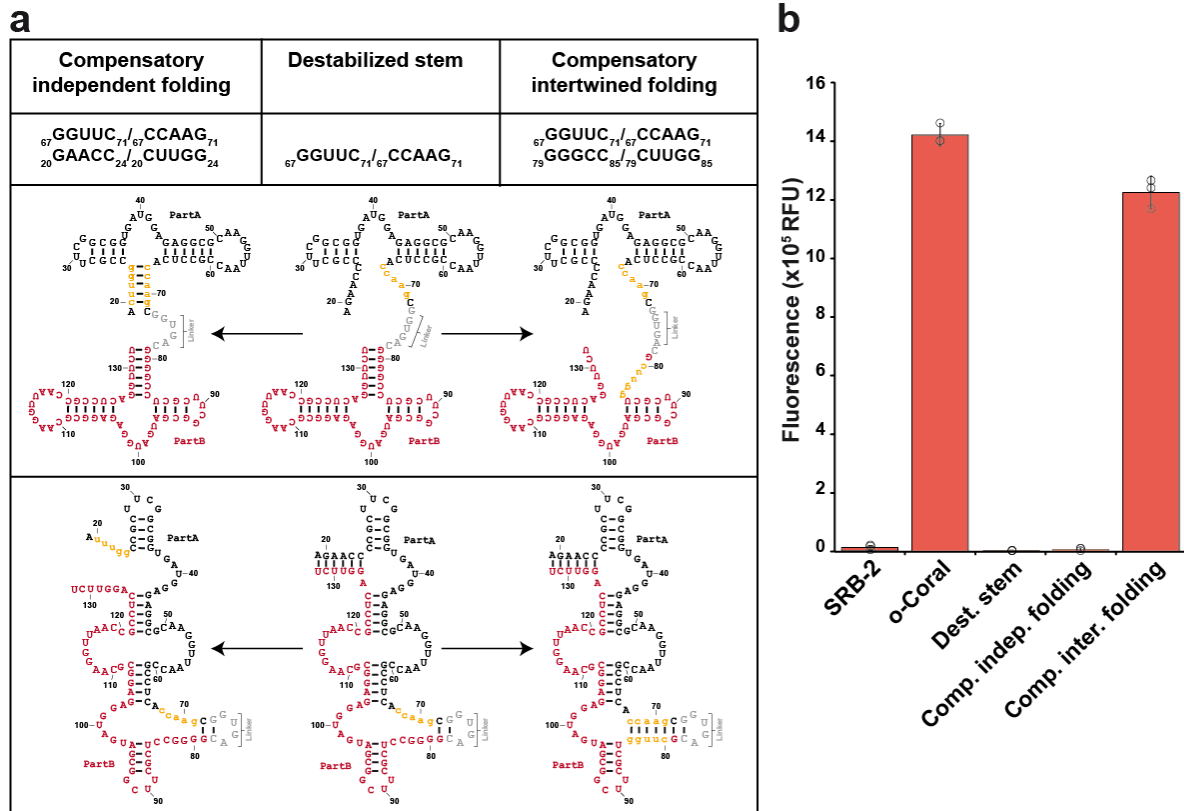
Supplementary Figure 4 | Sequence and fluorogenicity of the mutants isolated upon the *in vitro* evolution process. Variant sequences were ordered according to their Gemini-561 activation capacity normalized to that of SRB-2 (Norm. Fluo.). Mutations are color-coded (green, orange, red and blue for A, C, G and U respectively) and deletions represented by a “X”. Structural elements are delineated by shadowed areas and paired sequences indicated under the alignment. The clone ID refers to the round of selection from which the clone was extracted (first number) and the clone number (second number) assigned during the final screening. The presence of a linker and its size are indicated between both SRB-2 derived monomers. The gene coding for each mutant was transcribed *in vitro* in the presence of 100 nM of Gemini-561 and the fluorescence monitored. The fluorescence apparition rate was computed for each library and normalized to that of the parental SRB-2 aptamer. Please note that 5’ and 3’ constant regions are not represented. As a consequence, the numbering is downshifted by 18 nucleotides in comparison with the full-length molecule encompassing the 18-nucleotide long 5’ extension.



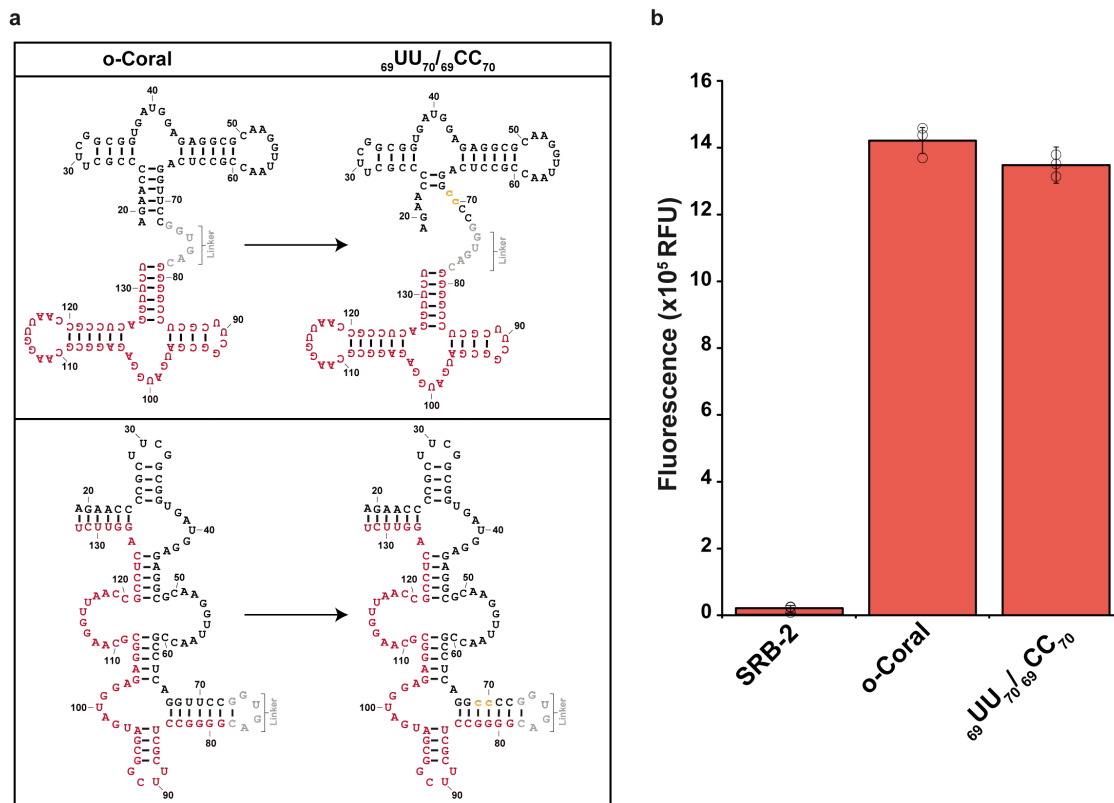
Supplementary Figure 5 | Probing of o-Coral secondary structure. (a) Probing experiment. Radioactively labeled o-Coral RNA was subjected to digestion by V1, T1 or T2 nucleases prior to analyzing the digestion products on 10 % polyacrylamide denaturing gels. The increased concentration of the enzymes is schematized by the colored triangles (V1: 0.001 U/ μ L – 0.002 U/ μ L – 0.004 U/ μ L, T1: 0.25 U/ μ L – 0.5 U/ μ L – 1 U/ μ L, T2: 0.0125 U/ μ L – 0.025 U/ μ L – 0.05 U/ μ L). Ctrl lane corresponds to an enzyme-free experiment, AH stands for Alkaline Hydrolysis in which o-Coral was statistically hydrolyzed, dT1 stands for denaturing T1 cleavages. The numbers on the right refer to o-Coral nucleotides. (b) Secondary structure model of o-Coral. T1, T2 and V1 cleavage sites are indicated respectively by the blue, green and red arrows. SRB-2 derived monomers are shown in black or red (Part A and B), whereas constant regions and linker are shown in gray. Acquired mutations found to contribute to o-Coral function are circled in black.



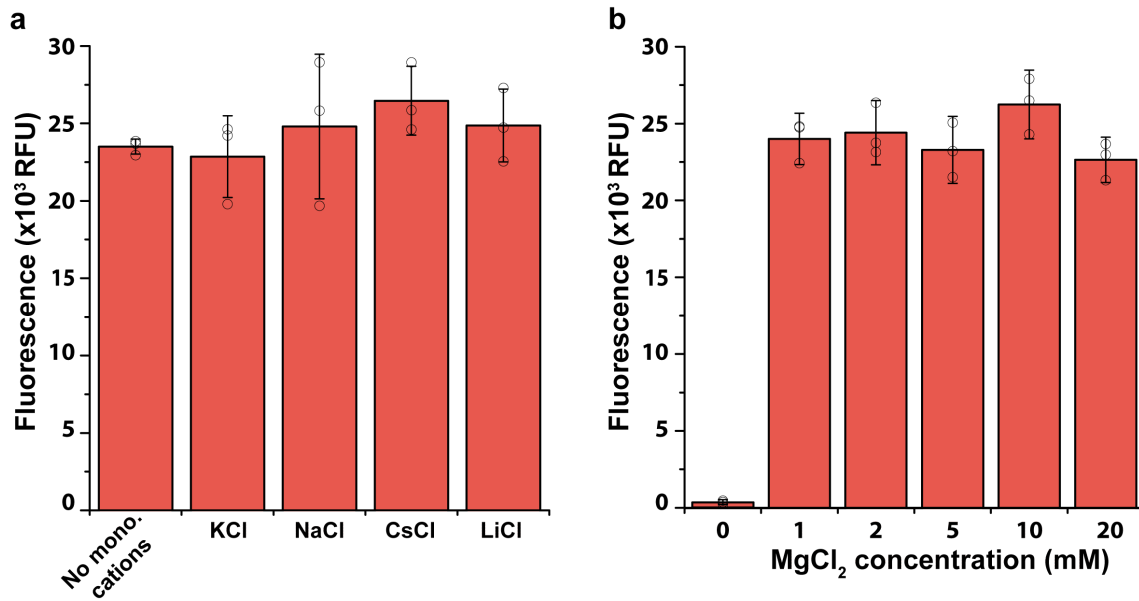
Supplementary Figure 6 | Secondary structure models of o-Coral aptamer. (a) Independent folding model. In this model, each SRB-2-derived monomer adopts an independent folding and closely resemble the original SRB-2 molecule associated by single stranded linker region. (b) Intertwined folding model. In this model, both each SRB-2 derived monomers fold on each other and form an intertwined structure. On both models, SRB-2 derived monomers are shown in black or red (Part A and B), whereas constant regions and linker are shown in gray. Acquired mutations found to contribute to o-Coral function are shown are circled in black.



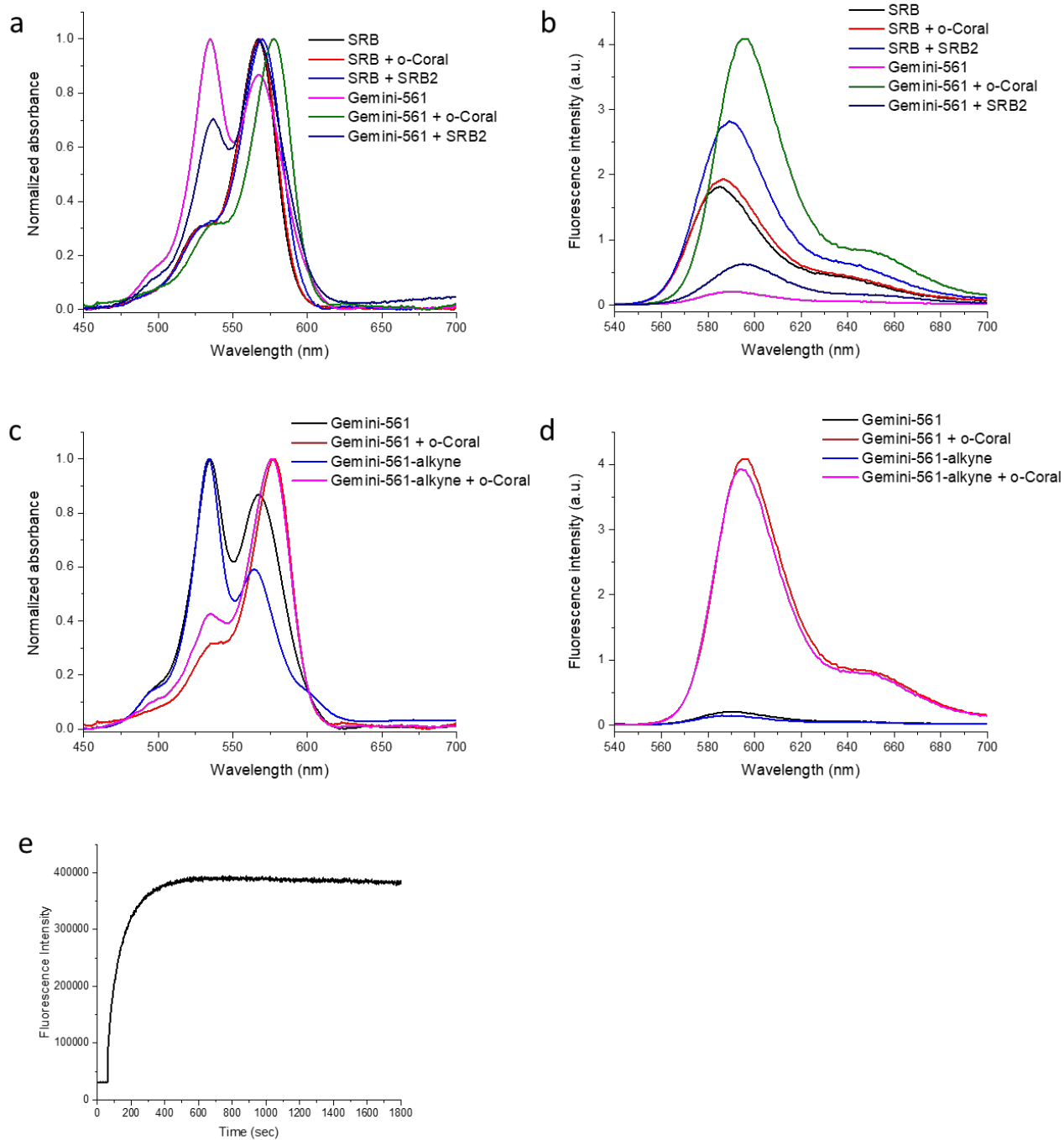
Supplementary Figure 7 | Refinement of structural model using P1 compensatory mutants. (a) Three mutants were generated: a destabilized mutant (Destabilized stem: ${}_{67}\text{GGUUC}_{71}/{}_{67}\text{CCAAG}_{71}$) of o-Coral and two potentially compensatory mutants; the first one based on the independent folding model (${}_{67}\text{GGUUC}_{71}/{}_{67}\text{CCAAG}_{71-20}\text{GAACC}_{24}/{}_{20}\text{CUUGG}_{24}$) and the second one based on the intertwined folding model (${}_{67}\text{GGUUC}_{71}/{}_{67}\text{CCAAG}_{71-79}\text{GGGCC}_{85}/{}_{79}\text{CUUGG}_{85}$). SRB-2 derived sequences (Part A and B) are shown in black or red whereas the linker sequence is shown in grey. Implemented mutations described before are shown in orange. **(b)** Impact of implemented mutations on o-Coral aptamer fluorogenicity. 500 nM of RNAs were incubated with 50 nM of Gemini-561 and the fluorescence was measured at $\lambda_{\text{ex/em}} = 560/600$ nm. The values are the mean of $n = 3$ independent experiments, each measurement being shown as an open circle. The error bars correspond to ± 1 standard deviation.



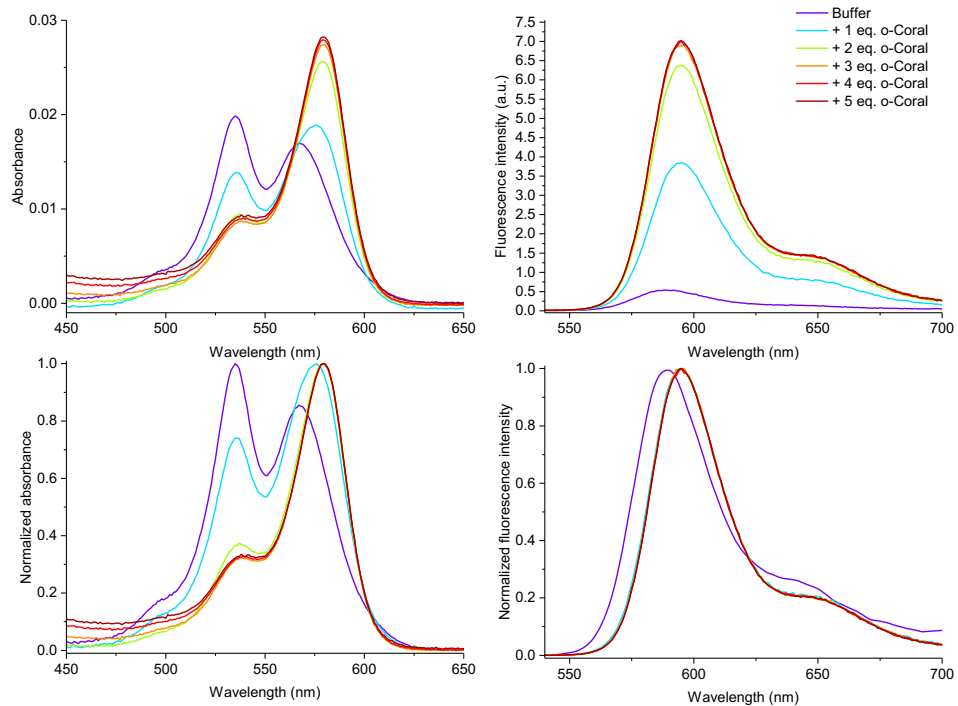
Supplementary Figure 8 | Refinement of structural model using CC double mutant. (a) Representation of o-Coral and the ${}_{69}\text{UU}_{70}/{}_{69}\text{CC}_{70}$ o-Coral double mutant according to the independent folding model (upper part) and the intertwined folding model (lower part). SRB-2 derived sequences (Part A and B) are shown in black or red whereas the linker sequence is shown in grey. Implemented mutations described below is shown in orange. (b) Impact of the implemented mutation on o-Coral aptamer fluorogenicity. 500 nM of RNAs were incubated with 50 nM of Gemini-561 and the fluorescence was measured at $\lambda_{\text{ex/em}} = 560/600$ nm. The values are the mean of $n = 3$ independent experiments, each measurement being shown as an open circle. The error bars correspond to ± 1 standard deviation.



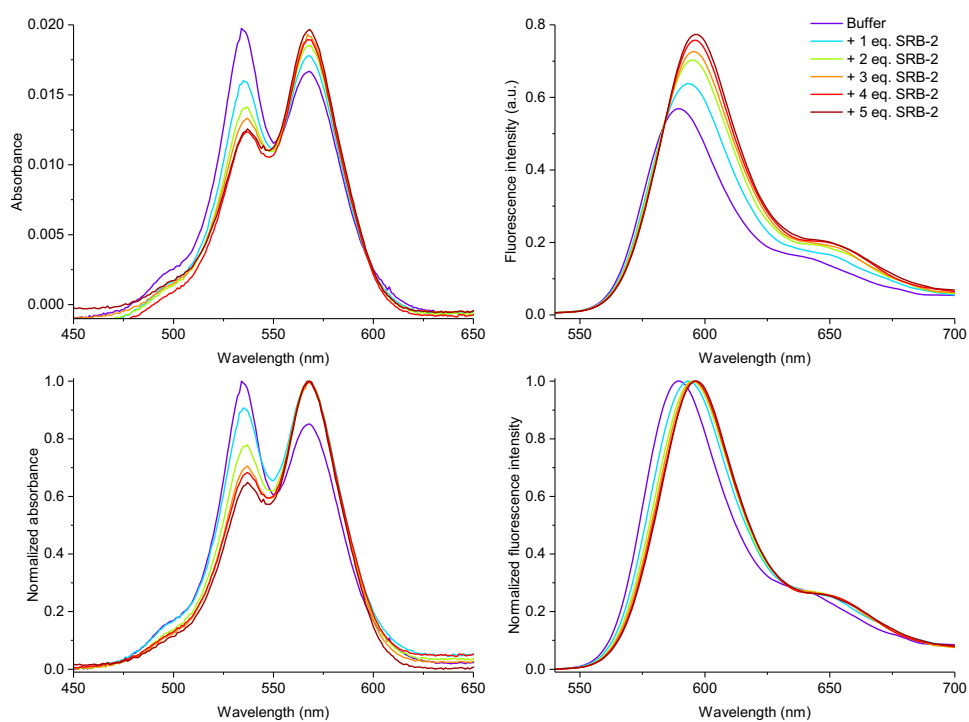
Supplementary Figure 9 | Salt dependency of Gemini561/o-Coral module. (a) Monovalent ions dependency of o-Coral. o-Coral RNA and Gemini-561 were mixed in a solution containing 40 mM Phosphate buffer pH7.5, 100 mM KCl or NaCl or CsCl or LiCl or in the absence of monovalent cations, 2 mM MgCl₂ and 0.05% Tween-20 and the fluorogenic capacity was measured. (b) Magnesium dependency of o-Coral. o-Coral RNA and Gemini-561 were mixed in a solution containing 40 mM Phosphate buffer pH7.5, 100 mM KCl, the indicated concentration of MgCl₂ and 0.05% Tween-20 and the fluorogenic capacity was measured. For both condition (a and b), 500 nM of RNAs were incubated with 50 nM of Gemini-561 and the fluorescence was measured at $\lambda_{ex/em} = 560/600$ nm. The values are the mean of $n = 3$ independent experiments, each measurement being shown as an open circle. The error bars correspond to ± 1 standard deviation.



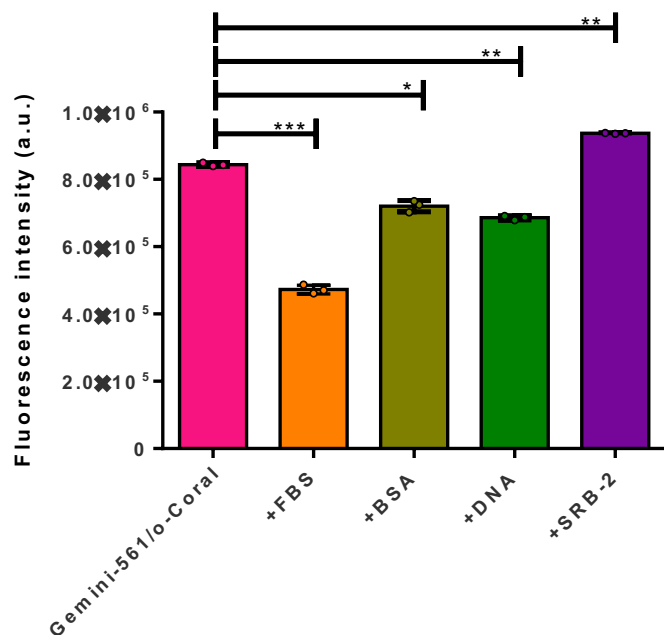
Supplementary Figure 10 | (a) Normalized absorption and (b) emission spectra of Gemini-561 or SRB (200 nM) in absence and in the presence of different RNA aptamers (600 nM). (c) Normalized absorption and (d) emission spectra of Gemini-561 or Gemini-561-alkyne (200 nM) in absence and in the presence of o-Coral (600 nM). Results were found similar in $n = 3$ independent experiments. (e) Kinetics of interaction between Gemini-561 (100 nM) and o-Coral (300 nM) measured as emission intensity at 586 nm as a functional of time. Excitation wavelength was 530 nm in all cases.



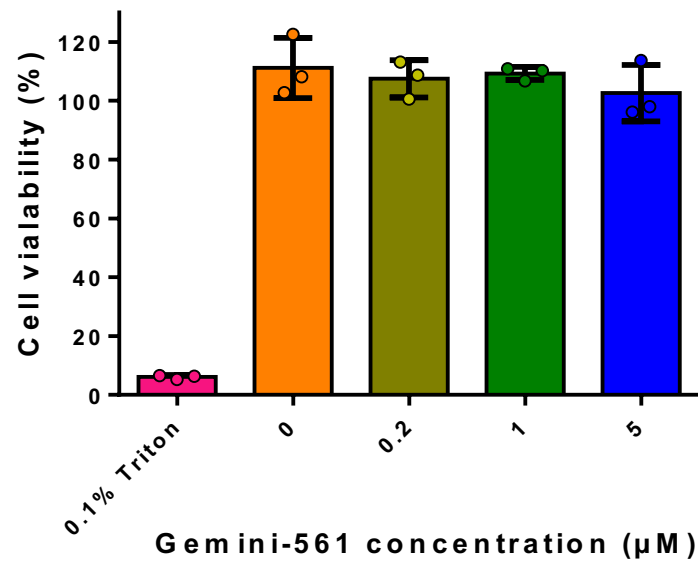
Supplementary Figure 11 | Absorption and emission spectra of Gemini-561 (200 nM) in the presence of increasing concentrations (equivalents, eq.) of o-Coral. Excitation wavelength was 530 nm. Measurements were performed once.



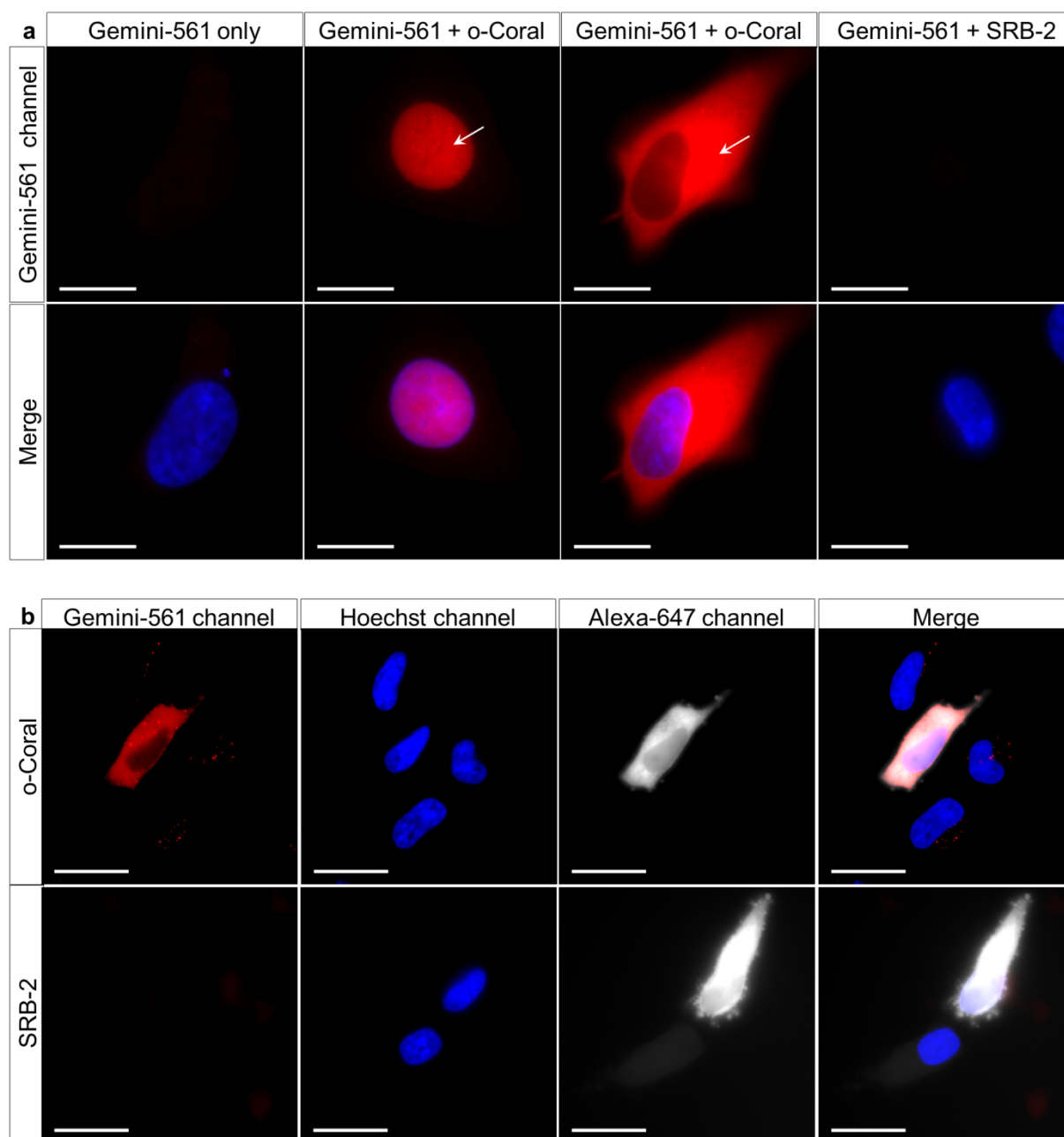
Supplementary Figure 12 | Absorption and emission spectra of Gemini-561 (200 nM) in the presence of increasing concentration (equivalents, eq.) of SRB-2 aptamer. Excitation wavelength was 530 nm. Measurements were performed once.



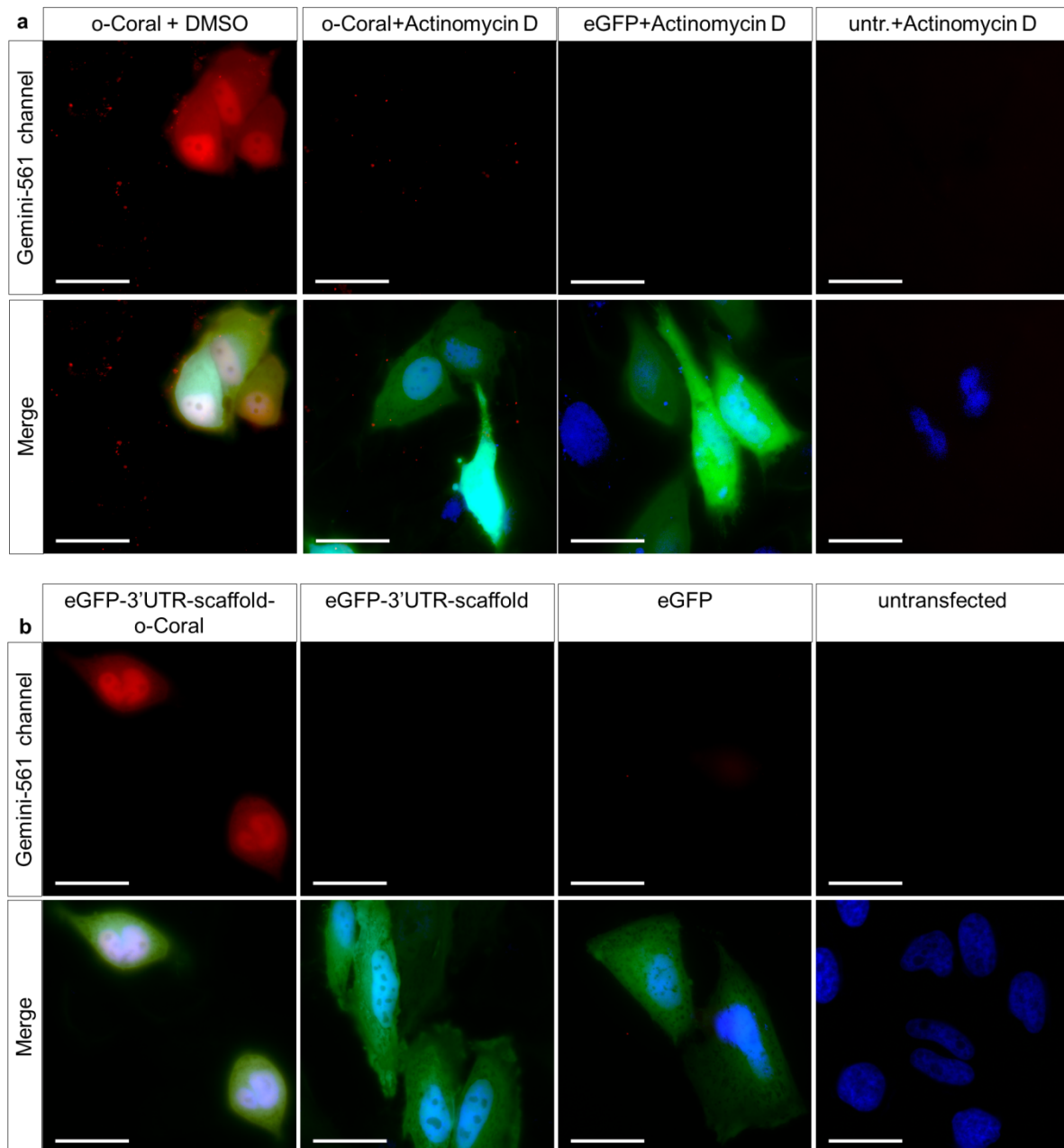
Supplementary Figure 13 | Effect of biomolecules and biological medium on the fluorescence intensity of Gemini-561/o-Coral (1/1 molar ratio) complex at 0.2 μM concentration. After Gemini-561/o-Coral complex was formed, the mixture was incubated with the corresponding biomolecule (BSA 10 mg/mL, non-targeted DNA 50 μM or SRB-2 aptamer 0.2 μM) or biological medium (FBS 10%) for 15 min and the fluorescence was recorded at 596 nm. Excitation wavelength was 530 nm. The values are the mean of $n = 3$ independent experiments, each measurement being shown as a colored dot. The error bars correspond to ± 1 standard deviation. Statistical significance based on ANOVA analysis: * $p > 0.05$; ** $p < 0.05$; *** $p < 0.001$.



Supplementary Figure 14 | Cytotoxicity assay of Gemini-561. HeLa cells were incubated with various concentration of Gemini-561 and their viability was assessed after 24 hours using MTT test. An incubation with 0.1% Triton X100 was used as negative control. The values are the mean of $n = 3$ independent experiments, each measurement being shown as a colored dot. The error bars correspond to ± 1 standard deviation.

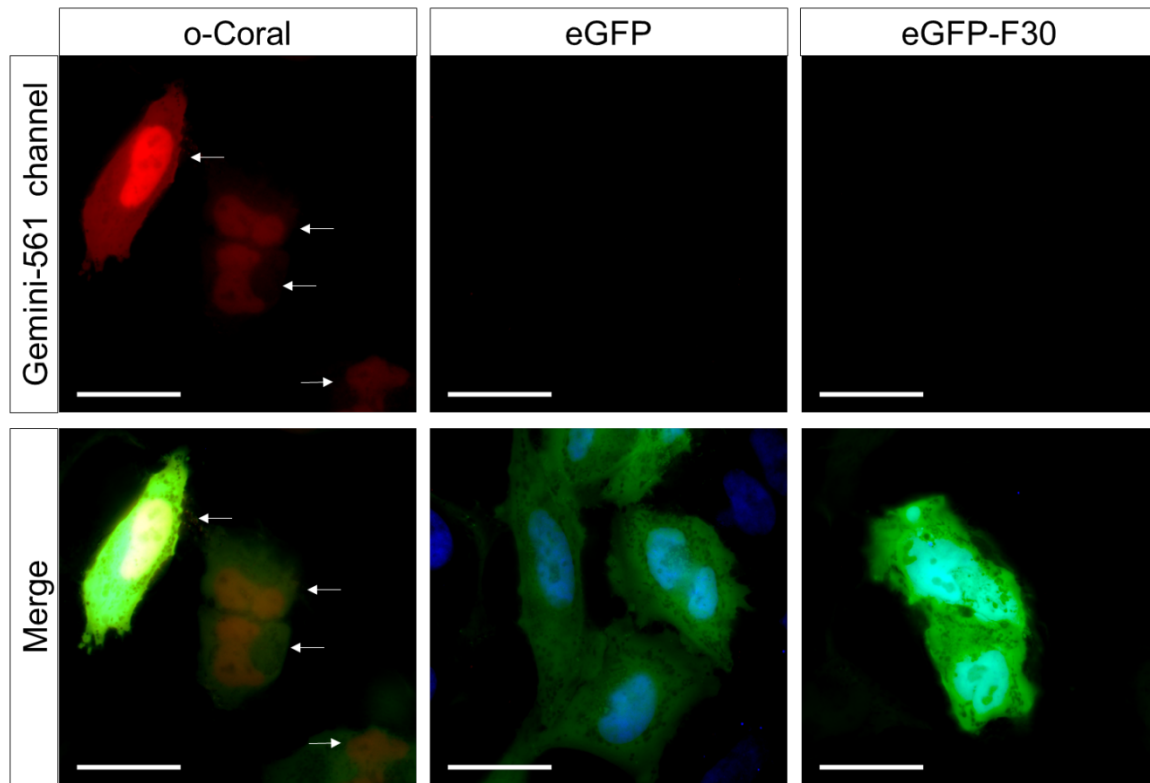


Supplementary Figure 15 | Microinjection in HeLa cells. (a) Microinjection of Gemini-561 ($1 \mu\text{M}$) alone (in cytosol), complex of Gemini-561/o-Coral ($1 \mu\text{M}$) or Gemini-561/SRB-2 ($1 \mu\text{M}$) (in cytosol). Arrows show that Gemini-561/o-Coral complex was microinjected into either nucleus or cytosol. Scale bar is $20 \mu\text{m}$. (b) Microinjection of o-Coral ($52 \mu\text{M}$) or SRB-2 ($52 \mu\text{M}$) with Dextran-Alexa-647 conjugate ($10 \mu\text{M}$) in cells pre-treated with Gemini-561 (200 nM) for 5 min. Microinjection parameters: $P_i=90 \text{ [hPa]}$; $T_i=0.3 \text{ [s]}$; $P_c=10 \text{ [hPa]}$. The nucleus was stained with Hoechst ($5 \mu\text{g/mL}$). The images were acquired using a 10s exposure time. Gemini-561 in red (ex: 550 nm , em: $595 \pm 40 \text{ nm}$), Hoechst in blue (ex: 395 nm , em: $510 \pm 42 \text{ nm}$) and Alexa-647 in white (ex: 638 nm , em: $810 \pm 90 \text{ nm}$). Scale bar is $30 \mu\text{m}$. Results were found similar in $n = 3$ independent experiments.



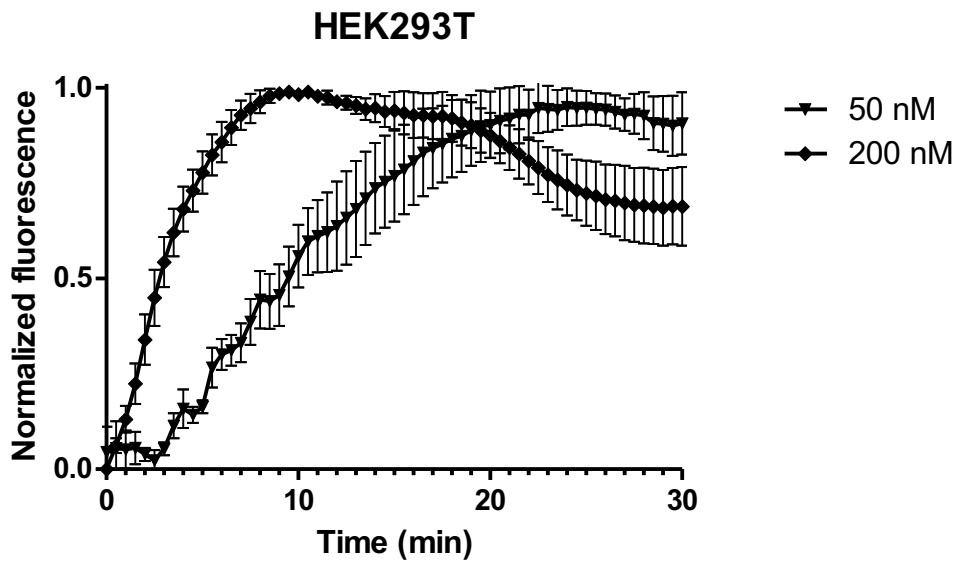
Supplementary Figure 16 | Live-cell imaging of o-Coral expressed from pol. II and pol. III promoter.

(a) Live cell imaging of HeLa cells expressing o-Coral from the U6-promoter in the absence and presence of Actinomycin D, cells expressing eGFP only and untransfected (untr.) cells treated with Actinomycin D. (b) Live cell imaging of HeLa cells expressing the *gfp* mRNA labelled with single copy of o-Coral. Cells expressing the *gfp* mRNA with or without scaffold inserted and untransfected cells were used as negative controls. (a-b) Cells were incubated with Gemini-561 (200 nM) for 5 min before imaging. Hoechst was used to stain the nucleus (5 μ g/mL). The images were acquired using a 500 ms exposure time. Gemini-561 in red (ex: 550 nm, em: 595 \pm 40 nm), Hoechst in blue (ex: 395 nm, em: 510 \pm 42 nm) and eGFP in green (ex: 470 nm, em: 531 \pm 40 nm). Results were found similar in n = 3 independent experiments. Scale bar is 30 μ m.

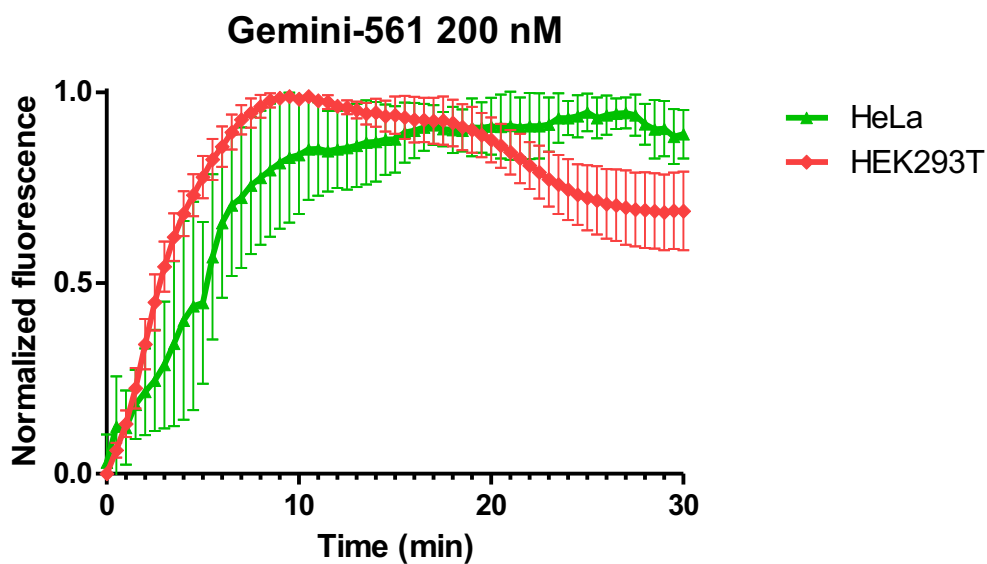


Supplementary Figure 17 | Live-cell imaging of transfected HeLa cells expressing eGFP and o-Coral, eGFP only or eGFP and F30 scaffold only. Top panel shows Gemini-561 channel only. Bottom channel shows merged all channels. Cells were incubated with Gemini-561 (200 nM) for 5 min. White arrows on the images depict the correlation between expression of eGFP and o-Coral as well as the different transcription states of cells. The images were acquired using a 500 ms exposure time. Gemini-561 in red (ex: 550 nm, em: 595±40 nm), Hoechst in blue (ex: 395 nm, em: 510±42 nm) and eGFP in green (ex: 470 nm, em: 531±40 nm). Results were found similar in n = 3 independent experiments. Scale bar is 30µm.

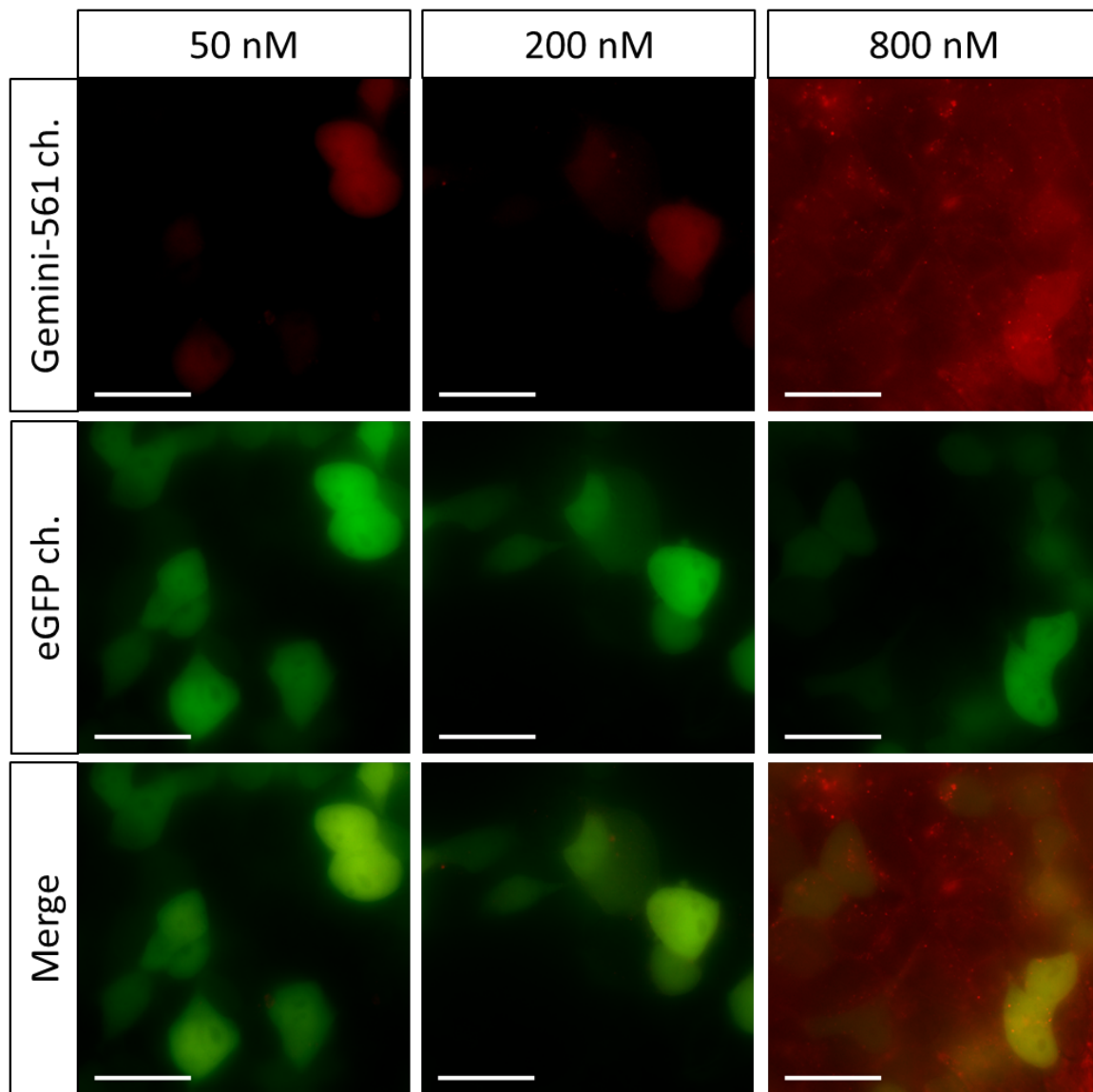
a



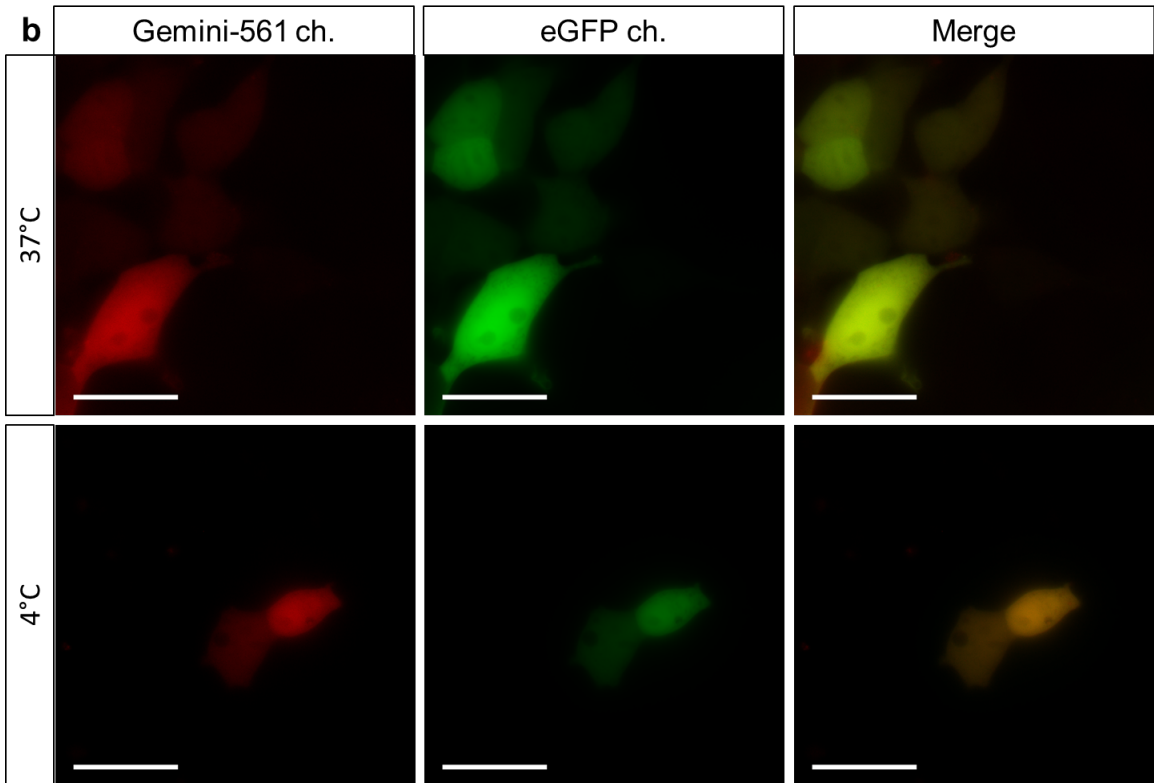
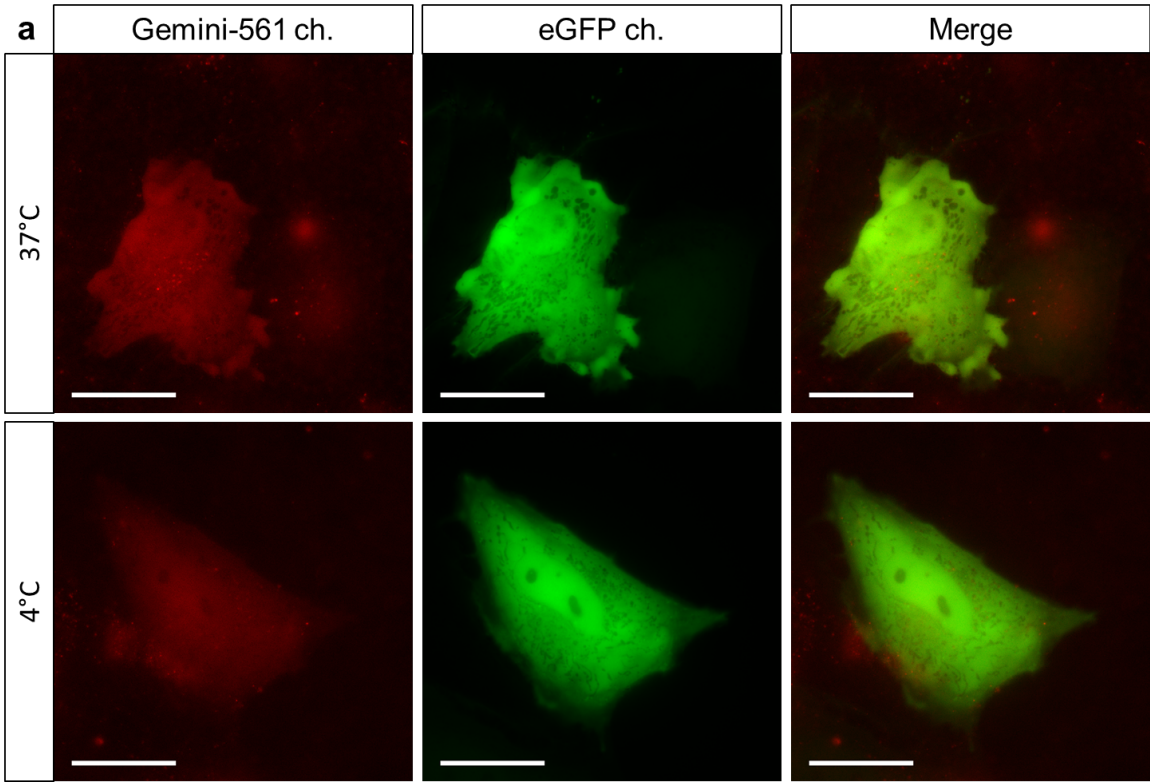
b

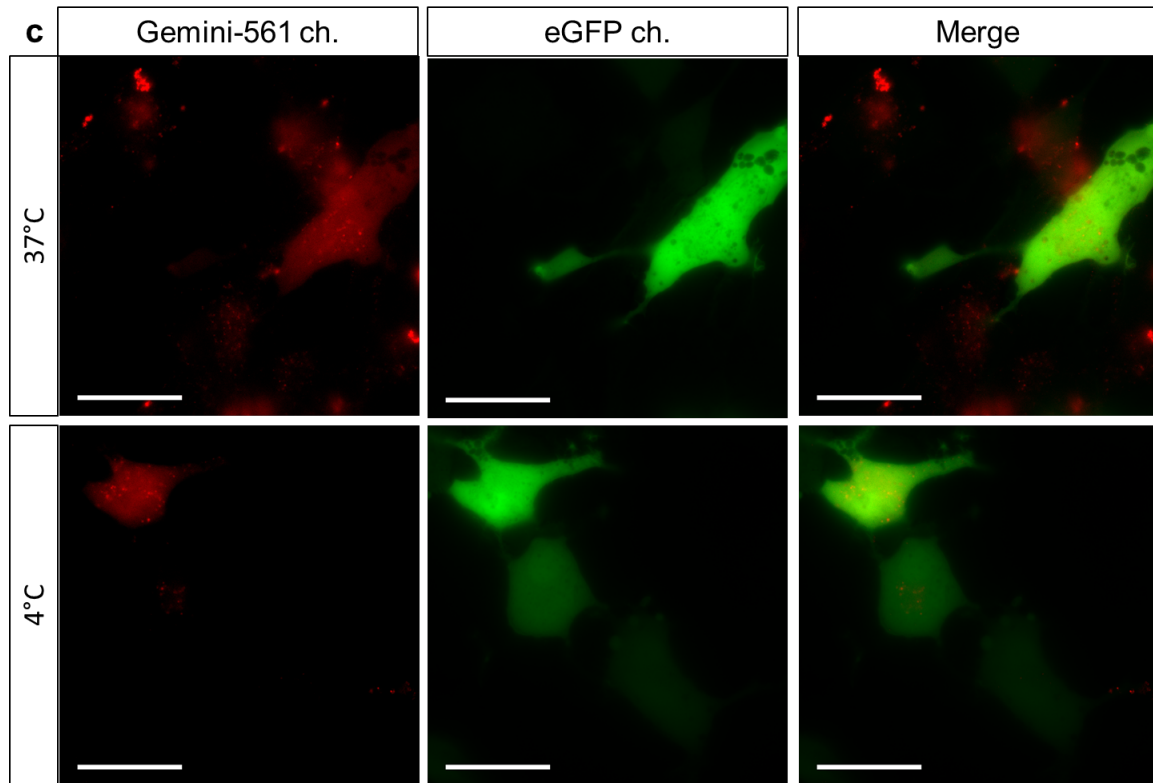


Supplementary Figure 18 | Kinetic studies of Gemini-561 uptake in *U6-o-Coral*-expressing live cells. (a) Concentration effect (50 nM and 200 nM) on Gemini-561 uptake in *U6-o-Coral*-expressing HEK293T cells. (b) Cell line effect (HeLa, HEK293T) on Gemini-561 (200 nM) uptake. Data represent average values of Gemini-561/*o-Coral* fluorescence intensity normalized to the maximum \pm 1 S.D. extracted from images ($n=6$). Experiments were independently performed at least 3 times.

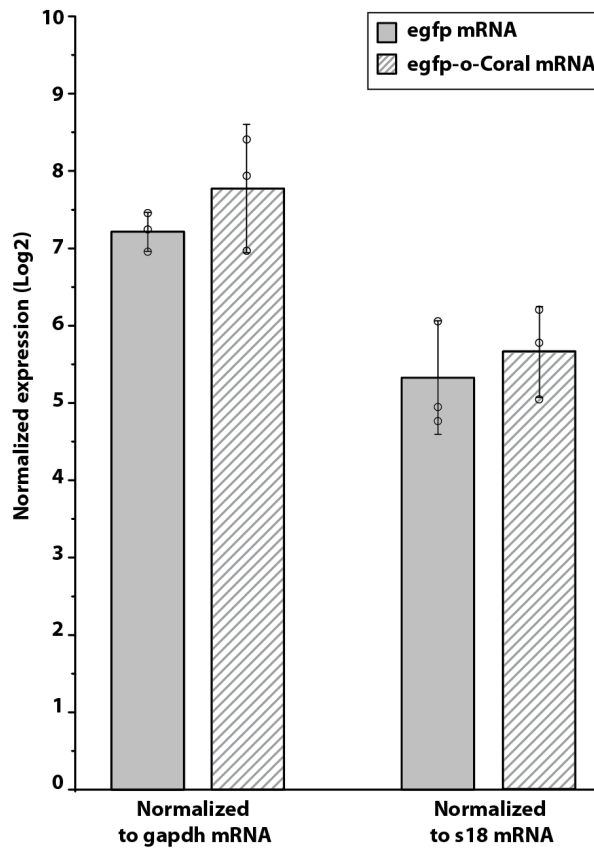


Supplementary Figure 19 | Live cell imaging of HEK293T cells expressing o-Coral from the U6-promoter, incubated for 5 min with Gemini-561 at concentrations 50 nM, 200 nM, 800 nM. The images were acquired using a 500 ms exposure time. Gemini-561 in red (ex: 550 nm, em: 595±40 nm) and eGFP in green (ex: 470 nm, em: 531±40 nm). Results were found similar in n = 3 independent experiments. Scale bar is 30 μ m.

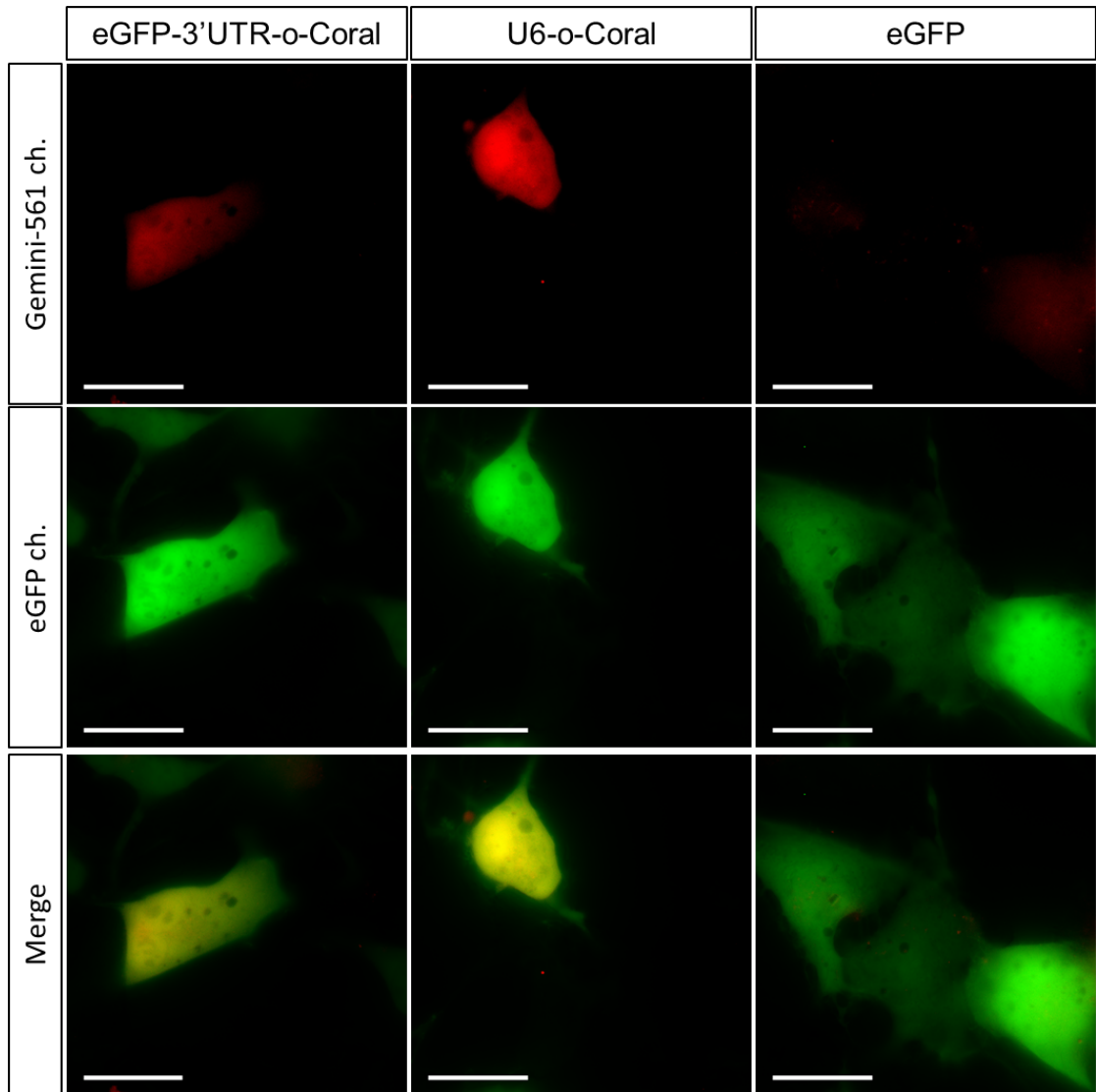




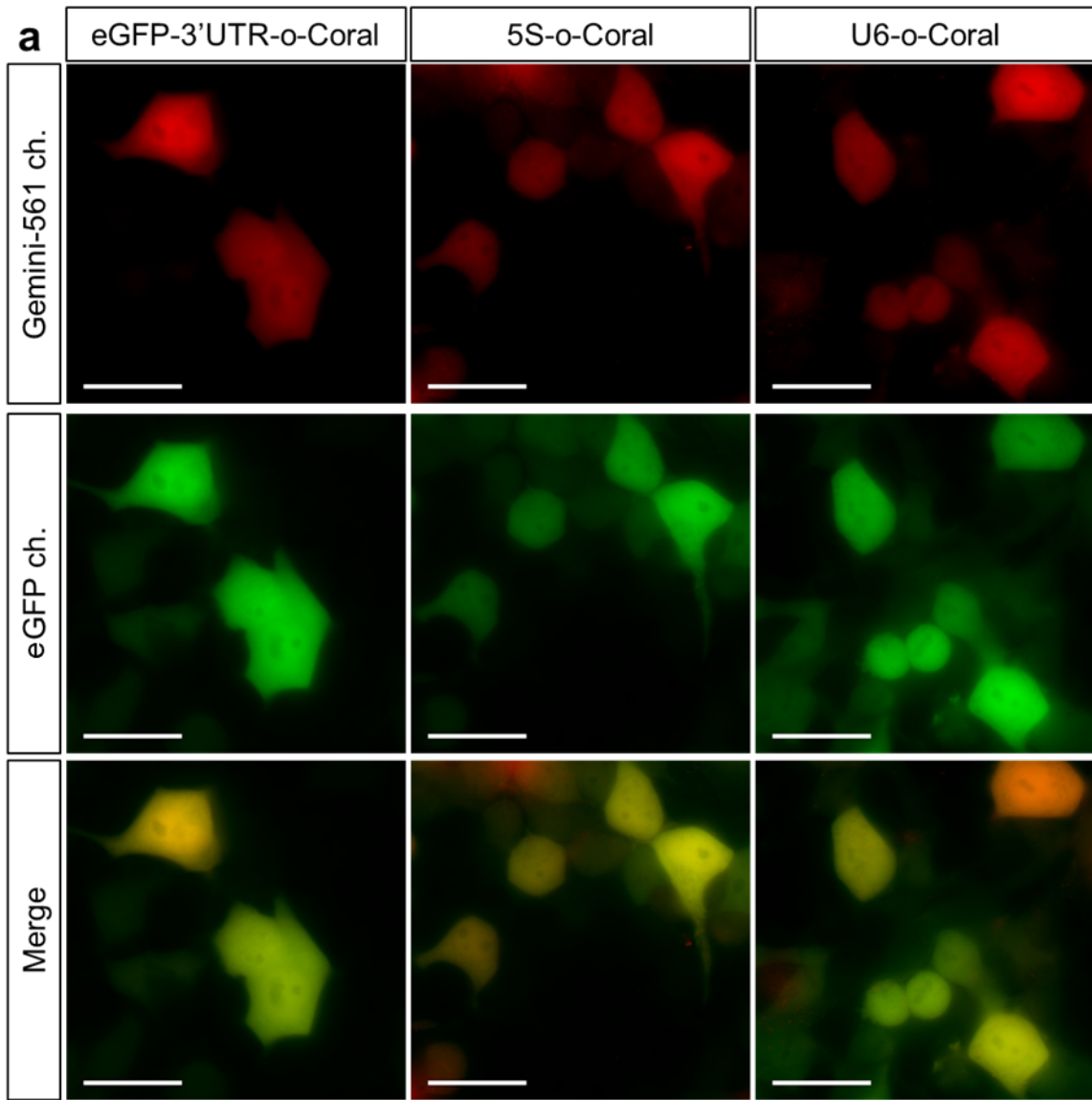
Supplementary Figure 20 | Effect of temperature on Gemini-561 internalization. Fluorescence imaging of HeLa (a), HEK293T (b) and U87 (c) cells expressing the U6-o-Coral, incubated for 5 min with Gemini-561 (200 nM) at 4 °C or 37 °C. (a-c) The images were acquired using a 500 ms exposure time. Gemini-561 in red (ex: 550 nm, em: 595±40 nm) and eGFP in green (ex: 470 nm, em: 531±40 nm). Results were found similar in n = 3 independent experiments. Scale bar is 30µm.

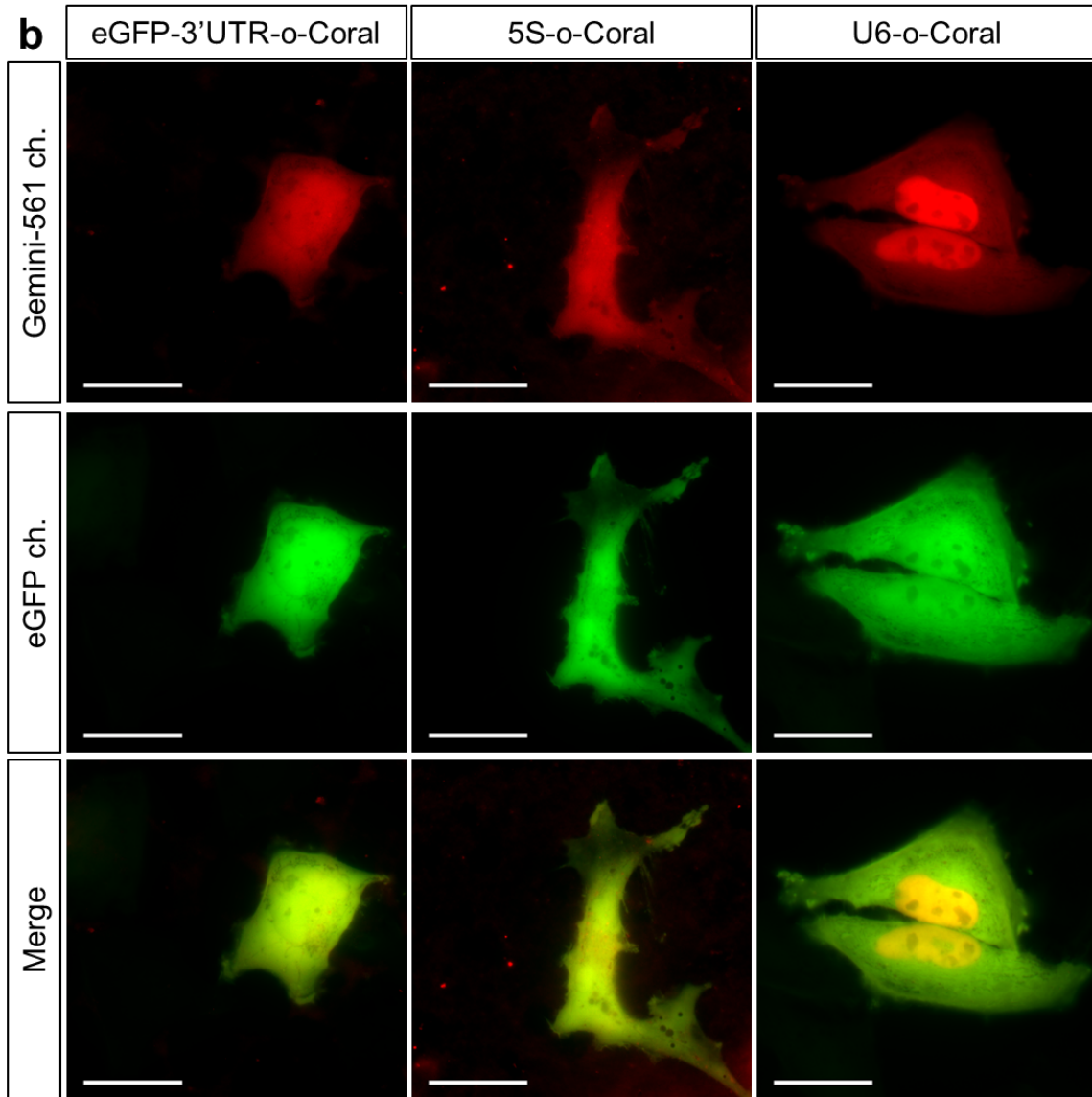


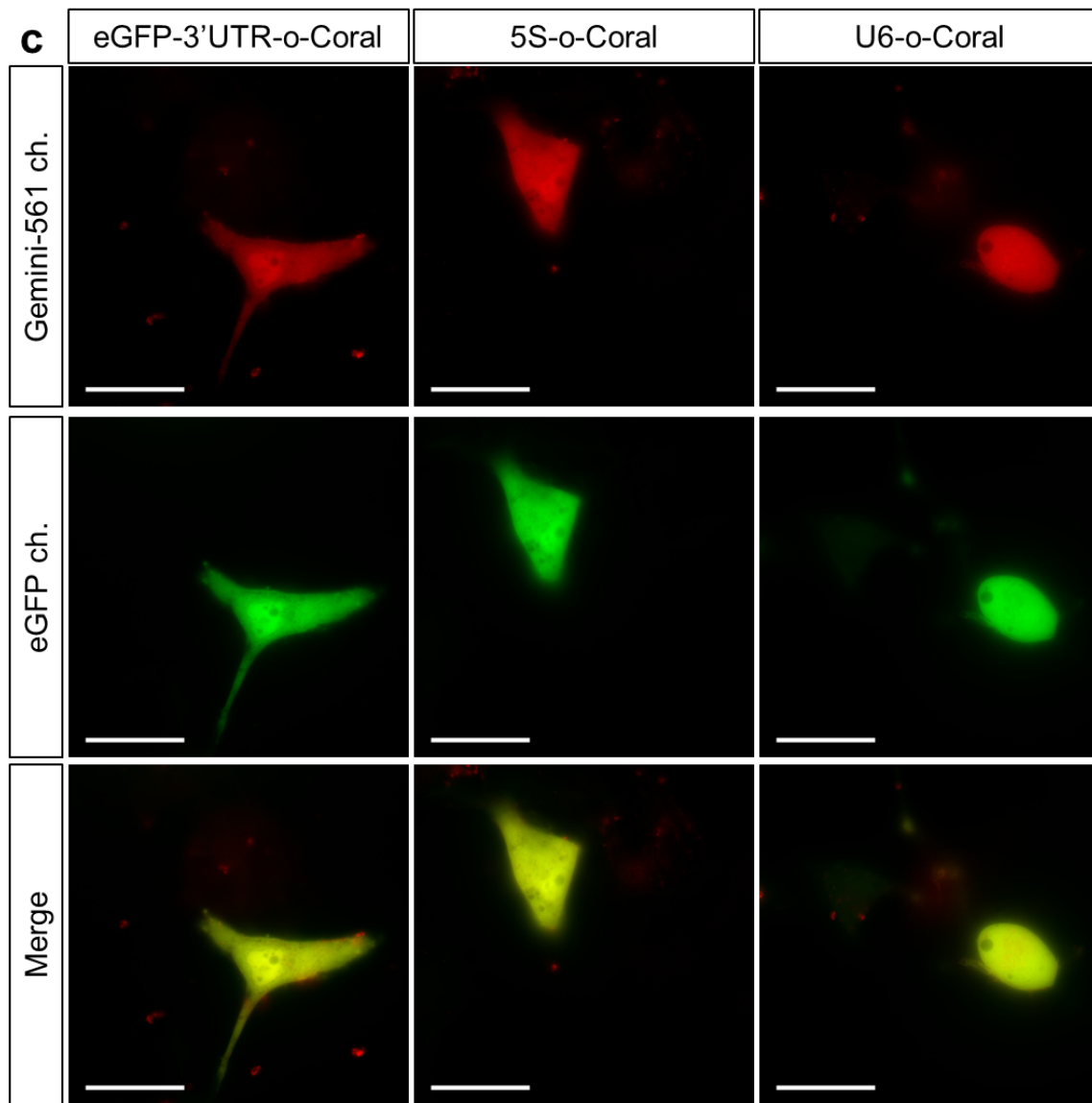
Supplementary Figure 21 | Effect of o-Coral on egfp mRNA level in the cells. Cells were transfected with a plasmid carrying a eGFP-coding gene containing (egfp-o-Coral) or not (egfp) o-Coral in the 3' untranslated region. Upon growth, cells were harvested and their content in gfp or gfp-o-Coral mRNA was quantified and normalized to that of two internal references: gapdh or s18 mRNA. The values are the mean of $n = 3$ independent measurements performed on three different batches of cells and the error bars correspond to \pm one standard deviation.



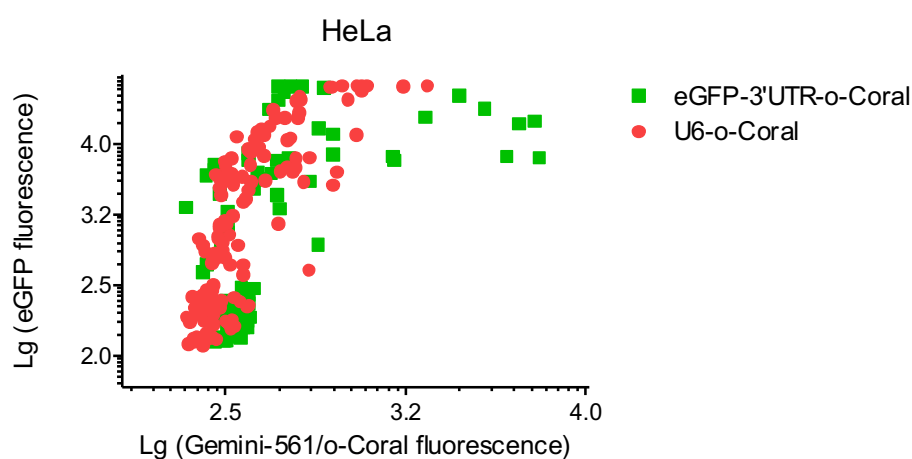
Supplementary Figure 22 | Fluorescence imaging of U87MG cells expressing the egfp mRNA labelled with a single copy of o-Coral in the 3'-untranslated region (3' UTR-o-Coral), o-Coral from the U6-promoter or eGFP only. Results were found similar in n = 3 independent experiments. Scale bar is 30 μ m.





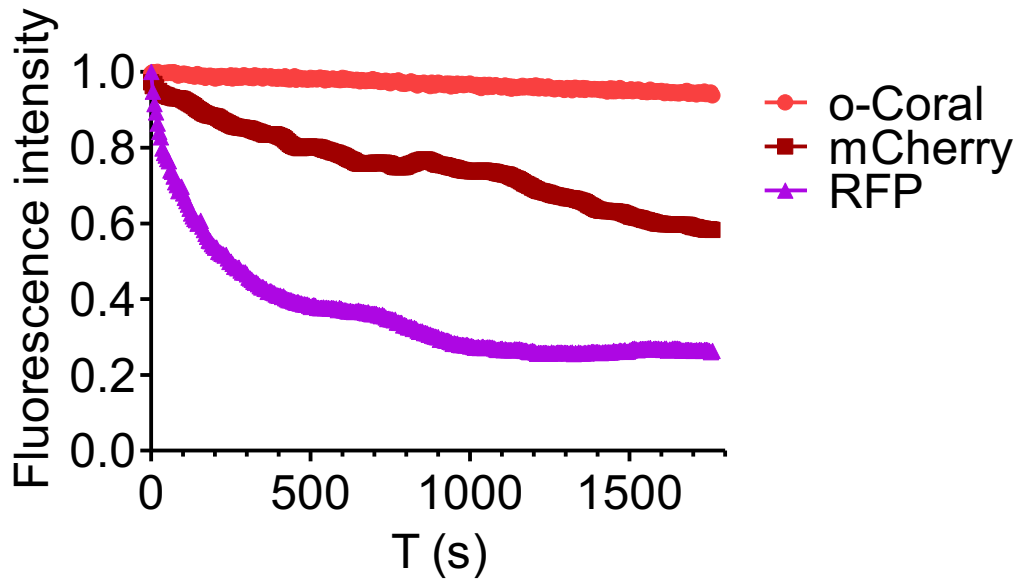


Supplementary Figure 23 | Live cell imaging of three different RNA constructs in three cell lines. HEK293T (a) HeLa (b) and U87MG (c) cells expressing the eGFP-3'UTR-o-Coral, 5S-o-Coral or U6-o-Coral, incubated for 5 min with Gemini-561 (200 nM). The images were acquired using a 500 ms exposure time. Gemini-561 in red (ex: 550 nm, em: 595±40 nm) and eGFP in green (ex: 470 nm, em: 531±40 nm). Results were found similar in n = 3 independent experiments. Scale bar is 30µm.

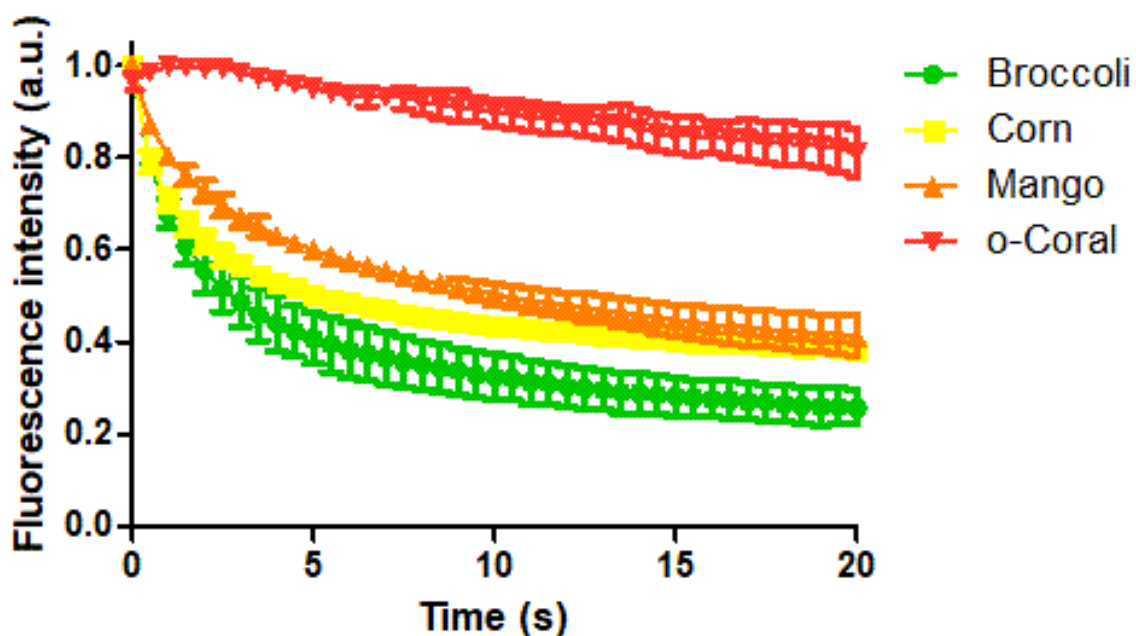
a**b**

Parameter	o-Coral	egfp_3'UTR_o-Coral
Number of XY Pairs	131	82
Pearson r	0.7996	0.5781
95% confidence interval	0.7279 to 0.8540	0.4129 to 0.7065
P value (two-tailed)	< 0.0001	< 0.0001
P value summary	****	****
Is the correlation significant? (alpha=0.05)	Yes	Yes
R square	0.6394	0.3342

Supplementary Figure 24 | (a) Correlation between fluorescence signal from eGFP with that from Gemini-561 in a single cell analysis of U6-o-Coral and egfp-3'UTR-o-Coral expressing HeLa cells. Each point represents the fluorescence signals from a single cell. (b) The table shows the results of the correlation analysis. Inbuilt two-tailed XY correlation analysis in GraphPad Prism was used with confidence interval 95% and data assumed to be sampled from Gaussian population (Pearson). The number of cells for o-Coral and eGFP_3'UTR_o-Coral were 131 and 82 respectively.

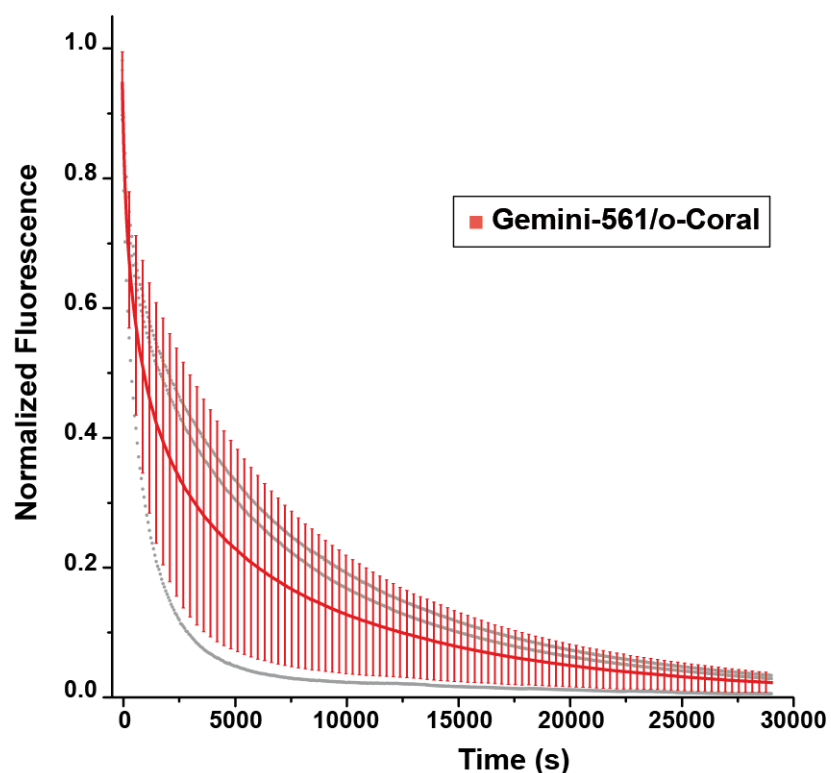


Supplementary Figure 25 | Comparative analysis of photostability by spectroscopy. Photostability of Gemini-561/o-Coral ($0.2 \mu\text{M}/1 \mu\text{M}$) compared to mCherry ($0.2 \mu\text{M}$) and RFP ($0.2 \mu\text{M}$). Each system was excited at the same molar extinction coefficient value: $30,000 \text{ M}^{-1} \text{ cm}^{-1}$. o-Coral, mCherry and RFP were excited using 532 nm laser (7 mW cm^{-2} , 18 mW cm^{-2} , 11 mW cm^{-2} respectively). Fluorescence intensity was monitored at 596 nm for o-Coral, 610 nm for mCherry and 584 nm for RFP. Experiment was repeated 2 times. Representative graph from 1 experiment is displayed.



Supplementary Figure 26 | Photostability of aptamer-dye couples in live HeLa cells.

Broccoli/DFHBI-1T, Corn/DFHO, Mango/TO1-biotin and o-Coral/Gemini-561 photostability was assessed by fluorescence microscopy. Cells were preincubated with corresponding dye (10 μ M DFHBI-1T, 10 μ M DFHO, 0.2 μ M TO1-biotin for 30 min and 0.2 μ M Gemini-561 for 5 min). Aptamers were microinjected in live HeLa cells at 20 μ M concentration. Microinjection parameters: $P_i=90$ [hPa]; $T_i=0.3$ [s]; $P_c=10$ [hPa]. Consecutive images were acquired, each using a 500-ms exposure time. Broccoli (ex: 470 nm, em: 475 \pm 50 nm); Corn (ex: 470 nm, em: 531 \pm 40 nm); Mango (ex: 470 nm, em: 531 \pm 40 nm); Coral (ex: 550 nm, em: 595 \pm 40 nm). The excitation power was adjusted to reach similar emission intensity. Fluorescence intensity values were extracted using same region of interest from 3 independent injections. The values are mean \pm S.D (n=3).



Supplementary Figure 27 | Photostability of Gemini-561/o-Coral over extensive constant illumination. A mixture of Gemini-561/o-Coral ($1 \mu\text{M}/2 \mu\text{M}$) was prepared and individualized into water-in-oil droplets to prevent unwanted exchange of complexes between illuminated and non-illuminated areas as described before in Fernandez-Millan, P., Autour, A., Ennifar, E., Westhof, E. & Ryckelynck, M. Crystal structure and fluorescence properties of the iSpinach aptamer in complex with DFHBI. *RNA* **23**, 1788-1795 (2017). The emulsion was then exposed to a constant illumination wavelength (575 nm) at the maximum intensity of the light source (Spectra X, Lumencor), and the emitted fluorescence (625 ± 50 nm) was collected by an Orca-Flash IV camera for 500 ms every 100 ms with $\times 40$ objective (numerical aperture (NA) 0.45). Individual measurements are shown in gray, whereas the mean values of the 3 independent experiments are shown in red. The error bars correspond to ± 1 standard deviation.